Tomographic visualization of thermo-diffusive instabilities of lean hydrogen/air mixtures

Goulier J, N'Guessan K, Idir M, Chaumeix N.
Institut de Combustion, Aérothermique, Réactivité et Environnement (ICARE), CNRS-INSIS
Orléans, France

1 Introduction

In case of a severe accident in a nuclear power plant with core meltdown, large amounts of hydrogen can be produced by the oxidation of the fuel sheathing with the cooling water or the interaction of the molten corium with the concrete and structure elements. Since hydrogen/air mixtures are characterized with very low ignition energy the presence of a hot surface may lead to ignition and propagation of a slow flame [1]. During its propagation, the flame can accelerate to a fast flame that can cause high pressure loads threatening the integrity of the containment building. Hence, it is mandatory to identify the phenomena that are responsible for this flame acceleration. Promptly after ignition, the surface of the flame wrinkles due to the Darrieus–Landau and the thermo-diffusive instability [2, 3]. The aim of this work is to characterize the wrinkling of the flame surface after ignition responsible for an early acceleration of the flame.

In order to measure the wrinkling of the flame surface, two complementary optical systems will be used, a Schlieren imaging system and a laser tomography. A Schlieren system is a non-intrusive technic based on the thermal gradient of the flame front where the observed flame is projected onto a screen (line of sight). Using Schlieren system, depth of the wrinkled flame surface is hidden [4]. Whereas laser tomography system allows us to observe a cross-section of a flame and therefore the depth of the wrinkles on the flame surface. On the other hand, tomography requires seeding which can impact the flame propagation.

This work will two aims: (i) to quantify the effect of seeding on the propagation of lean hydrogen/air flame, (ii) to estimate the surface of wrinkle of flame during its propagation.

2 Experimental Set-up

Measurements were performed on a new large spherical vessel with an inner diameter of 563 mm [5, 6]. The vessel can sustain a pressure up to 200 bar and temperature ranging from ambient temperature to 300 °C. Two tungsten electrodes mounted on the equatorial plan of the sphere are used to ignite the mixture using a high voltage discharge. Two pressure transducers (Kistler 6001 and 601A) are mounted, respectively on the top and bottom part of the vessel (with an angle of 42 ° from the equatorial plan), to record the pressure

Correspondence to: chaumeix@cnrs-orleans.fr

during the combustion. The chamber is equipped of 4 quartz windows of 200 mm of diameter used to visualize the flame during its propagation using either Schlieren system or laser tomography.

Visualization of the flame inside the chamber was made using a Z-shape Schlieren system coupled with a high-frequency camera. A white continuous lamp (300 W Xe Lot-Oriel) is used to illuminate the flame via a lens of focal 200 mm and two concave mirrors of focal 1.5 m. A high frequency camera (Phantom V1210) with an acquisition of 19 000 frames per second and resolution of 768 x 768 pixels², records the Schlieren images of the growing flame. The recorded images are the projection of the flame onto a screen.

Cross-section of the flame is obtain using laser tomography with a 15 W continuous laser at a wavelength of 532 nm (Verdi G15 Coherent Laser) with a seeding of Di-Ethyl-Hexyl-Sebacat of ~5 µm diameter. A 1 mm wide and 70 mm height laser sheet passing through the center of the vessel was generated using a combination of two semi-cylindrical lens. One diverging lens of focal 10 mm to widen the laser beam follow by a converging lens of focal 20 cm to limit the spread of the beam. Laser sheet is recorded using a Phantom V1210 at 19 000 frames per second with a resolution of 768 x 768 pixels^2. To ensure the necessary resolution for the detections of wrinkles, only the bottom half of the flame have been analyzed. Using the gradient of the greyscale level, the flame front position is detected on each image. The radius of the flame, r, is estimated by fitting a circle on the pixel detected. The center of the circle is fixed at the ignition point. The surface of an equivalent sphere with a smooth surface can be expressed as $A_S = 4\pi r^2$. Using the length of the flame front detected, l, and the angle between the first and the last point, θ, the surface of a wrinkle flame, A_W, can be expressed as:

$$A_W = 4\pi\left(\frac{l}{\theta}\right)^2 \tag{1}$$

Amplification factor of the surface, AF_{Surf}, is defined as the ratio of the surface of the wrinkle flame, A_W, with the equivalent surface of a smooth flame, A_S.

After the extraction process of the flame radius versus time of Schliren images, the spatial flame speed $V_S = \mathrm{d}r/\mathrm{d}t$ can be determined. However, owing to the spherical shape of the flame, the flame is curved and as such is subject to a stretch rate which in turns varies with the size of the flame. In the case of spherical expanding flames, the stretch rate, κ, is well defined and is given by the following expression:

$$\kappa = \frac{2}{r}V_S = \frac{2}{r}\frac{dr}{dt} \tag{2}$$

Thus it is necessary to apply a stretch correction to the velocity either using a linear extrapolation. The early analysis of Clavin [7] and Matalon [8] led to consider that, for a relatively weak stretch rate, the laminar flame speed varies linearly with the global stretch rate according to the following expression:

$$V_S = V_S^0 - L_b \cdot \kappa \tag{3}$$

where V_S^0 is the unstretched spatial flame speed, κ the stretch and L_b the Markstein length. L_b is a parameter characterizing the response of the flame when submitted to a given stretch. Using the unstretched spatial flame speed and the Markstein length, amplification of the flame speed can be define as the spatial flame speed divided by the flame speed of a smooth flame at a corresponding radius:

$$AF_{Speed} = \frac{V_S}{V_{S,Smooth}} = \frac{V_S}{V_S^0}\left(1 + \frac{2L_b}{r}\right) \tag{4}$$

The studied mixtures were constituted of hydrogen and air, the molar fraction of hydrogen varied from 0.16 to 0.28. The air was chosen of well-defined composition (Air Liquide, grade alphagaz 2, purity >99.9999%) with following composition: 20.9% O_2+ 79.1% N_2. The mixtures were prepared directly inside the vessel introducing the hydrogen last to avoid mass diffusion during the introduction of the air. Initial temperature at the inner wall and total pressure was fixed at 296 K and 1 atm respectively.

3 Impact of the droplets on the flame propagation

To assess the impact of the seeding on the flame propagation, laminar flame speed, V_S, was measure using the Schlieren system with or without the presence of droplets. The quantity of seeding introduced was the same as the one used for the tomographic experiments.

The evolution of the spatial flame speed, V_S, as a function of the radius of the flame, r, with or without seeding are presented on figure 1. With the addition of particles to the hydrogen/air mixture, the spatial flame speed oscillates between strong acceleration phase and week deceleration phase. For mixtures with 16 % of hydrogen in air, the spatial flame speed oscillates between an acceleration phase over 12 mm of radius growth and a deceleration phase over 5 mm of radius growth. Increasing the concentration of hydrogen in the mixture results in the elongation of the acceleration and deceleration phases. Those acceleration phases are not observed with mixture of 16 % and 20 % of hydrogen in air with seeding. For the seeded 24 % and 28 % of hydrogen in air, acceleration and deceleration phase are observed with oscillation at lower frequencies. Such oscillations, characteristic of flame surface instabilities, have been reported for very large scale flame of propane/air flames by Bauwens et al. [9]. These oscillations are found to be the result of periodic growth and saturation of a narrow range of length scales that follows each generation of cell formation.

The first acceleration phase, which is characteristic of the formation of thermo-diffusive instabilities, does not occurs at the same critical radius whether the mixture is seeded or not. Formation of instabilities occurs at lower radius for seeded mixtures of 24 % and 28 % of hydrogen in air. For the 28 % of hydrogen in air mixture, the difference between the first acceleration phase with or without seeding is 14 mm. For the 24 % of hydrogen in air, the difference is 8 mm. The same difference is very low for the 20 % and 16 % hydrogen in air mixtures.

One can notice that the spatial flame speed, before the apparition of instabilities, is lower for all the seeded mixtures by ~20 cm/s. This difference in the spatial flame speed might be due to the energy needed for the vaporization of the oil during the flame propagation.

Thus, adding seeding to the mixture modify the behavior of hydrogen/air flame propagation; (i) flame surface instabilities, that are responsible of the early flame acceleration phase, occur at lower radius; (ii) spatial flame speed is lowered by 20 cm/s before the apparition of instabilities; (iii) for radius above the critical radius of flame surface instabilities apparition, oscillatory behavior of the flame speed is more pronounced. However, the flame speed level with or without seeding are alike on the observation range making the use of tomography relevant to access the wrinkling of the flame surface.

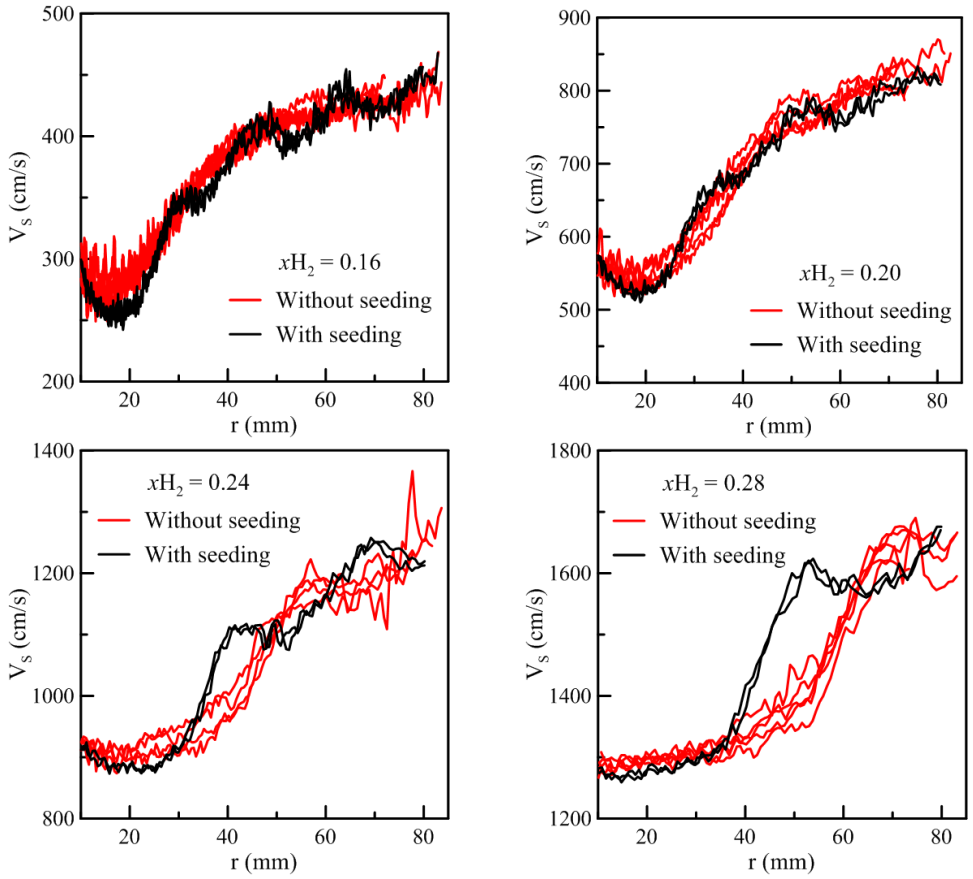

Figure 1. Impact of the seeding on the evolution of the spatial flame speed as a function of time for hydrogen/air mixture with a molar fraction of 0.16, 0.20, 0.24 and 0.28 at P_{ini} = 101 kPa and T_{ini} = 293 K.

4 Tomographic measurements

Though the flame propagation is impacted by the presence of droplets, amplification factor of the surface, AF_{Surf}, can be compared to the amplification factor of the speed, AF_{Speed}. Unstretched spatial flame speed, V_S^0 and Markstein length, L_b, were extrapolated linearly using the Schlieren observation with the addition of seeding. Amplification factor of the surface, AF_{Surf} and the speed, AF_{Speed}, are plotted as a function of the radius of the flame for four different molar fraction of hydrogen in air on the figure 2.

For each mixture, the measurement of the amplification factor of the surface, AF_{Surf} is highly scattered compared to the amplification factor of the speed, AF_{Speed}. The scattering is due to the error induced by the extrapolation of the total surface from a small portion of flame front. Nevertheless, for the 20 %, 24 % and 28 % of hydrogen in air, both amplification factor overlap with a given proportionality factor. For the 16 % of hydrogen in air, the amplification factor of the surface, AF_{Surf} is highly scattered after a radius of 40 mm.

Ratio of amplification factor of the speed, AF_{Speed}, with the amplification factor of the surface, AF_{Surf}, as a function of the hydrogen molar fraction is reported on the figure 3. For a 16 % of hydrogen mixture, the proportionality factor is 2 and decreases according to a second order polynomial to 1.29 for 28 % of hydrogen mixture.

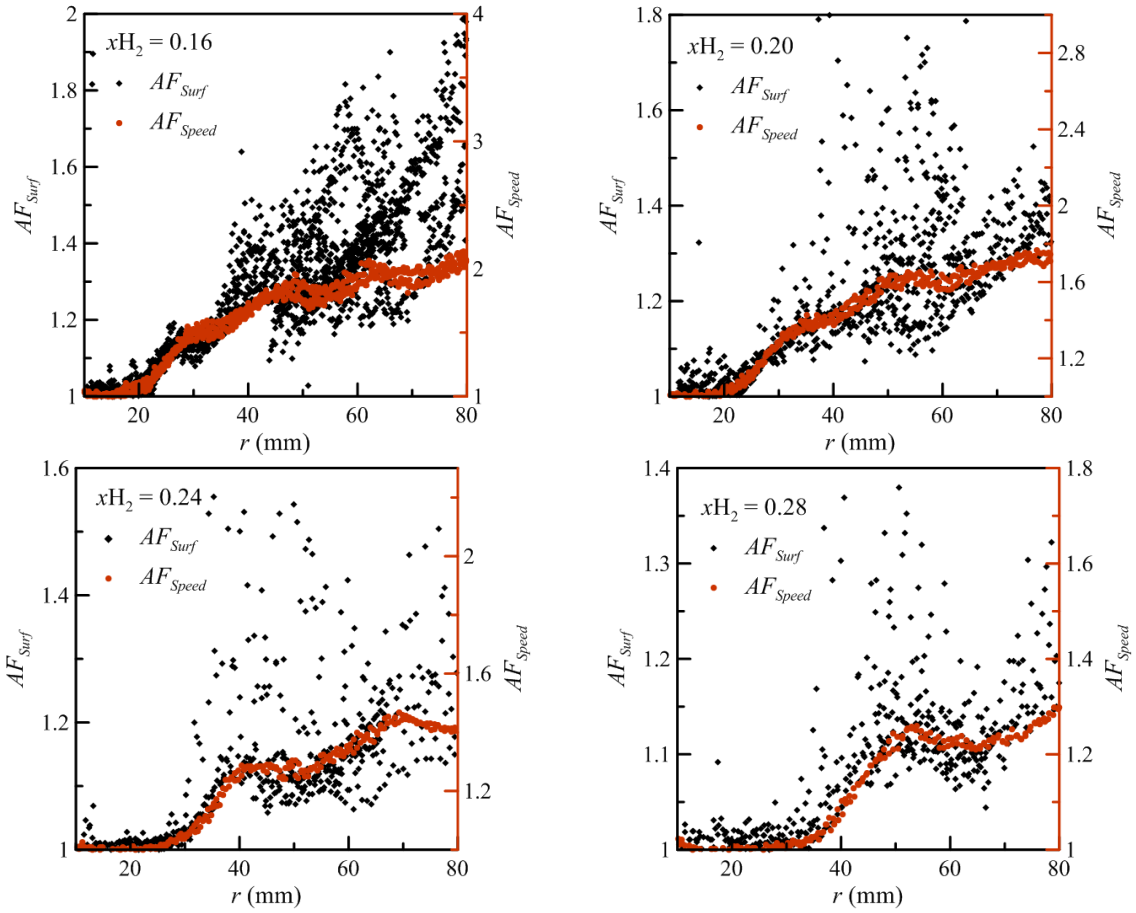

Figure 2. Comparison of the amplification factor of the speed, AF_{Speed}, with the amplification factor of the surface, AF_{Surf} for hydrogen/air mixture with a molar fraction of 0.16, 0.20, 0.24 and 0.28 at P_{ini} = 101 kPa and T_{ini} = 293 K.

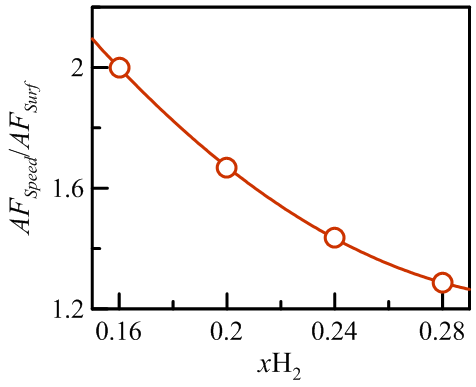

Figure 3. Ratio of the amplification factor of the speed, AF_{Speed}, with the amplification factor of the surface, AF_{Surf}, for hydrogen/air mixture with a molar fraction of 0.16, 0.20, 0.24 and 0.28 at P_{ini} = 101 kPa and T_{ini} = 293 K.

Value of the proportionality factor is given as a function of the molar fraction of hydrogen in the mixture using the polynomial equation:

$$\frac{AF_{Speed}}{AF_{Surf}} = 28.37(xH_2)^2 - 18.41xH_2 + 4.22 \qquad (5)$$

5 Conclusion

This study presented new results concerning the measurement of flame surface instabilities of lean to nearly stoichiometric hydrogen/air mixtures obtained using laser tomography. The addition of seeding to the mixture modify the behavior of the flame propagation, flame surface instabilities occur at lower radius, the spatial flame speed is lowered by 20 cm/s before the apparition of instabilities and for radius above the critical radius of flame surface instabilities apparition, oscillatory behavior of the flame speed is more pronounced.

Using laser tomography, we were able to assess the flame surface instabilities of large radiuses hydrogen/air wrinkled flames (r up to 80 mm). The amplification of the wrinkled flame surface was compared to the amplification of the flame velocity. The ratio

Both amplification where overlapping for a given proportionality constant dependent of the hydrogen molar fraction of the mixture.

References

[1] Drell IL, Belles FE. (1958). Survey of hydrogen properties.

[2] Darrieus G. (1938). Propagation d'un front de flamme. Communication présentée à La Technique Moderne.

[3] Landau LD. (1944). On the theory of slow combustion. Acta Physicochim URSS 19, 77–85.

[4] Bradley D, Haq MZ, Hicks RA, Kitagawa T, Lawes M, Sheppard CGW, Woolley R. (2003). Turbulent burning velocity, burned gas distribution, and associated flame surface definition. Combustion and Flame 133: 415-430.

[5] Goulier J, Chaumeix N, Halter F, Meynet N, Bentaïb A. (2016). Experimental study of laminar and turbulent flame speed of a spherical flame in a fan-stirred closed vessel for hydrogen safety application. Nucl. Eng. Des. (http://dx.doi.org/10.1016/j.nucengdes.2016.07.007).

[6] Goulier J, Comandini A, Halter F, Chaumeix N. (2016). Experimental study on turbulent expanding flames of lean hydrogen/air mixtures. Proc. Combust. Inst. (http://dx.doi.org/10.1016/j.proci.2016.06.074).

[7] Clavin P. (1985). Dynamic behavior of premixed flame fronts in laminar and turbulent flows. Prog. Energy Combust. Sci. 11: 1-59

[8] Matalon M, Matkowsky BJ. (1982). Flame as gasdynamic discontinuities. J. Fluid Mech. 124: 239-259

[9] Bauwens CR, Bergthorson JM, Dorofeev SB. (2015). Experimental study of spherical-flame acceleration mechanisms in large-scale propane–air flames. Proc. Combust. Inst. 35: 2059-2066